Title

Improving Vehicle Ride Comfort Through Seat Control Using Bond Graphs

Authors

Akbari, Ali

Margolis, Donald

Publication Date

2024-07-01

Peer reviewed

IMPROVING VEHICLE RIDE COMFORT THROUGH SEAT CONTROL USING BOND GRAPHS

Ali Akbari
Department of Mechanical and Aerospace Engineering, UC Davis, Davis, California, USA
Email: alakbari@ucdavis.edu

Donald Margolis
Department of Mechanical and Aerospace Engineering, UC Davis, Davis, California, USA
Email: dlmargolis@ucdavis.edu

ABSTRACT

In a paper published at the previous ICBGM conference, it was argued that having knowledge of the internal dynamics within the passenger's body could be attributed to their perception of ride comfort. Using the biomechanical model developed for this purpose, a novel, quantitative ride comfort metric is devised. Then the passenger model is exposed to the disturbance vibration coming in from a generic vehicle. A bond-graph representation of a full-car model is developed and the complete system, including the passenger, the seat, and the vehicle body as well as wheels and unsprung masses, is simulated. The nonlinear system of equations is linearized and an observer-based state-variable-feedback controller is designed. It is shown that with 3 sensors collocated with 3 actuators for seat control positioned at the rest locations on the seat, ride comfort can be improved significantly while maintaining little power consumption.

Keywords: Passenger Biomechanics, Ride Comfort, Bond Graph Modeling, Seat Control

1. INTRODUCTION

The concept of ride comfort in ground vehicles comfort is a major component in the development of vehicle dynamics. However, passenger comfort is conceptually a quality which cannot be directly measured. With the rise of autonomous vehicles and the competition for the market in the vehicle industry, passenger comfort is a vital concern for automotive manufacturers(Wang, Zhao et al. 2020). Therefore, passenger comfort must somehow be quantified such that it could be integrated into a vehicle design.

But how is that achieved? First one must notice that there are many qualitative factors that impact the perception of ride comfort, such as temperature, air quality, visual and auditory ques, and vibration(Da Silva 2002). Since this research is studying ride comfort from a mechanical engineering perspective, vibration is considered to be the sole agent responsible for ride comfort.

ICBGM'2024 July 1-3, 2024- San Diego, California USA - ©2024 Society for Modeling & Simulation International (SCS)

To quantify ride comfort, one straight-forward way is to perform tests on human subjects. However, there are not many passenger-comfort experiments available in the literature, especially those which have well accounted for various ages, physiques, and other subject-dependent criteria. Due to the subjectivity of what everyone may experience in the test, it is rather difficult to come up with a unique measure of ride comfort using passenger test data. Wang et al.(Wang, Zhao et al. 2020) stated that comfort can substantially enhance people's acceptance of autonomous vehicles and argued that ride comfort is mostly associated with vehicle's acceleration and that their comfort measure correlates most significantly with a linear combination of all four lateral/longitudinal acceleration/jerk signals. However, their comfort criterion has correlation discrepancies against gender and the direction of motion (longitudinal/lateral). Oborne(Oborne 1976, Oborne 1977) published a critical assessment of the available experimental studies on passenger comfort with respect to vertical vibrations and argued that said experimental tests were inconclusive and that their results have

barely benefited the design engineers as their multiple conclusions do not comply with one another. For instance, they point out that the same vertical acceleration in magnitude and frequency (0.01g at 10 Hz) was perceived quite differently in the available ride comfort studies within the literature, ranging from "more than uncomfortable"(Jacklin 1936) to "Just above threshold"(Dieckmann 1958) and "almost very good"(Sperling and Betzhold 1957).

Yang et al.(Yang, Ren et al. 2009) reviewed several published experiments on vibration comfort. In their rather extensive research, it was found that the available literature is discrepant when it comes to determining ride comfort levels. They argued that a peak acceleration value of 0.3 m/s^2 corresponded to conflicting indications of comfort amongst the various sources including "almost uncomfortable"(Reiher and Meister 1932), "almost perceptible"(Fothergill and Griffin 1977), "comfortable"(Oborne and Clarke 1974), "not uncomfortable"(Jones and DJ 1974, Sharma 2016), and "very unsatisfactory"(Enders, Burkhard et al. 2019).

Multiple studies, the most recognized of which being the ISO2631(ISO 1997), rely on the premise that acceleration is the proper measure of ride comfort where the smaller the acceleration, the more comfortable the ride. The ISO2631 is an ISO standard on human whole-body vibrations that chooses acceleration as the responsible agent for ride comfort and suggests frequency weighting filters for the acceleration signal in the vertical, lateral, and longitudinal directions to account for humans' perception of vibration intensity. Afterwards, a net value of the filtered acceleration signal is calculated and cross-referenced with the ranges given by ISO2631 for thresholds of comfort(ISO 1997).

The US Army Tank Automotive Center conducted an experiment led by Pradko and Lee in 1966 where in a passenger test, they urged that the passengers' perception of ride comfort did not correlate well with acceleration data, whereas it agreed rather promisingly with data for "Average Absorbed Power", a quantity that is proportional to the square of the acceleration signal (similar to a power spectral density) with a proportionality constant that is only frequency-dependent and is constant for any individual frequency(Pradko and Lee 1966). This research culminated in an industrial standard known as Adjusted Absorbed Power or AAP which states that a ride is comfortable as long as the adjusted absorbed power remains below 6 Watts. Besides ISO2631 and AAP, other industry-adopted ride comfort standards include the acceleration-based VDI-2057 from Germany(VDI 2002), and the acceleration-based BS-6841 from the UK(BSI 1987). In a study to investigate the applicability of the four aforementioned established industrial standards to ride comfort in off-road vehicles, Els(Els 2005) argued that while the four ride comfort standards had similar predictions for conservative ride conditions and that they agreed on the trend that higher acceleration exacerbates the perception of ride comfort, they did not agree on ride comfort thresholds, as a ride scenario could be perceived as comfortable according to one standard and uncomfortable according to another. Amongst Els' findings was another keen observation: their study shows that ride comfort is subjective, as the same ride had been perceived differently among people who had different occupations, such that the managers had rarely found a ride comfortable whereas soldiers rarely found one uncomfortable.

Judging from the aforementioned studies and how their introduced metrics for passenger comfort are in partial defiance of one another, it can be concluded that a universal ride comfort index does not yet exist and that currently established indices are prone to subjective discrepancies.

Much like cold being merely the absence of heat, comfort seems to virtually be the lack of discomfort. If the human body undergoes vibrations which would make it feel uncomfortable, that will have to be felt as the result of a nervous connection transmitting signals of pain/discomfort. Since the body's musculoskeletal system (the body's internal mechanical domain) is essentially responsible for "taking in" and "feeling" said input motions to the body, any motion-induced discomfort must correspond to a nervous signal coming from the musculoskeletal system. And those nerves in turn are associated with "changes" within the musculoskeletal system which are in fact the body's internal dynamics.

The author hereby claims that knowledge of the internal dynamics of the body in response to the

disturbance input vibrations correlates with the nervous signals which "feel" the input motion and therefore constitute one's perception of comfort/discomfort. Hence, it is proposed that through modeling the body's internal dynamics in response to the input motions from a vehicle, one could determine whether said ride is comfortable or not. The author hypothesizes that if the body's internal mechanics are adequately modeled, one can correlate its response to input vibration with feelings of discomfort. If motions from the internal dynamics model exceed their respective comfortable range of motion, this will signify discomfort. In other words, one could describe a most comfortable ride as one that during which the least amount of internal motion/reaction is induced within the human body; and that the higher the levels of internal motion/reaction, the higher the discomfort.

To address the lack of a ubiquitous ride comfort index, a quantitative ride comfort metric will be developed that can estimate the effect of input vibrations on the passenger's body and make a comfort inference according to its internal, dynamic response. Should such a metric be available, one can associate controllable vehicle outputs with ride comfort and develop vehicle control algorithms accordingly or design vehicle systems to achieve maximum ride comfort. This provides the motivation for developing a biomechanical model of a vehicle's passenger. This model should be sufficiently sophisticated to include the necessary degrees of freedom while still not being too complicated to prevent intuition. Henceforth this proposed biomechanical model will be known as the Passenger Model. A subsequent vehicle model will be built and the passenger model will be subjected to vibrations coming in from a vehicle model as it traverses a random road. A novel ride comfort metric will be devised according to passenger biomechanics and finally, a controller will be designed which will optimize the introduced ride comfort metric.

2. MODELING

The modeling effort includes the development of the passenger model, the vehicle model, the ride comfort metric, and the controller design.

2.1. PASSENGER MODEL

The passenger model has been developed in a previous study with the aid of bond graphs (Akbari and Margolis 2021, Akbari and Margolis 2024). Fig.1 shows a schematic of the passenger model.

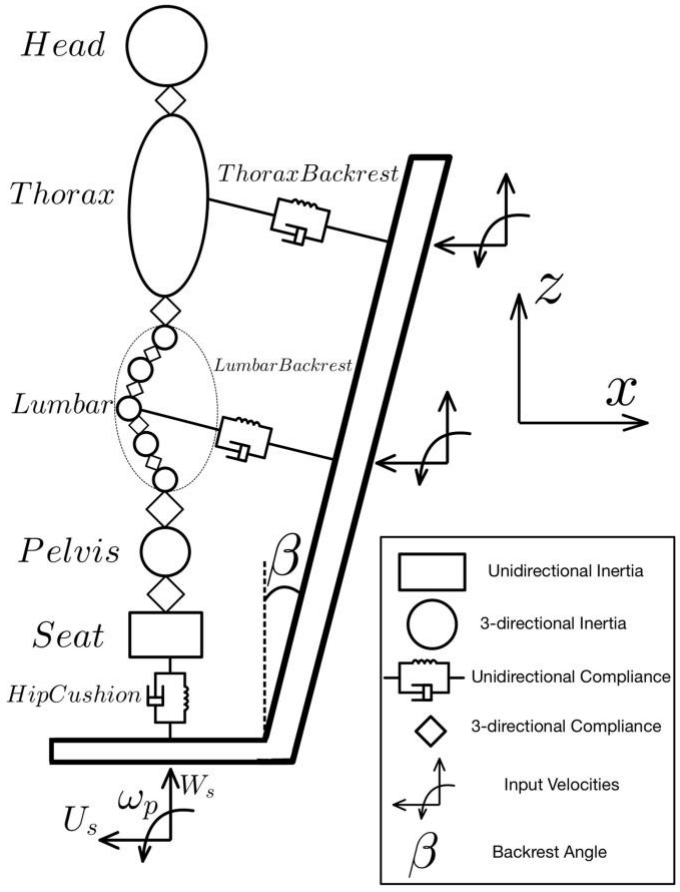

Figure 1. Schematic of the passenger model

With the passenger model at hand, a vehicle model is required to calculate the input vibrations from the vehicle to the passenger model.

2.2. VEHICLE MODEL

A full-car model is developed using bond graphs. Fig. 2 displays a schematic of the vehicle model.

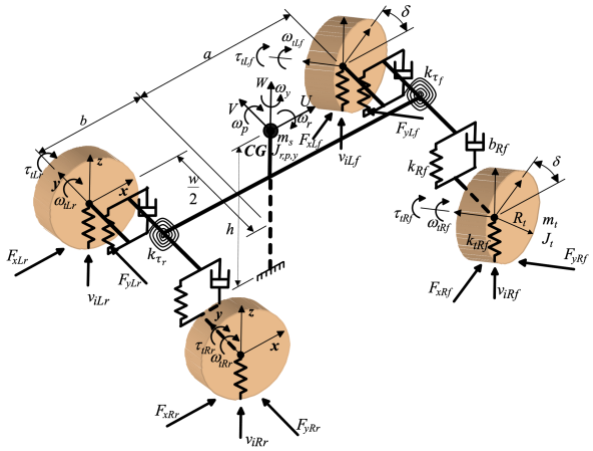

Figure 2. The full car model

The employed vehicle model belongs to a 4-corner vehicle with suspension units in each corner and with front and rear anti-roll bars. The inputs to the vehicle model are the front steered wheels' angle and the road input below each corner. The bond graph for the vehicle model excluding the anti-roll bars is given in Fig.3.

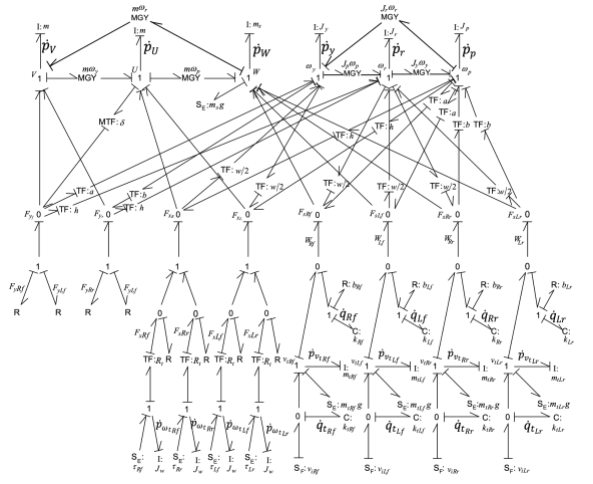

Figure 3. Full car model bond graph

The anti-roll bar has not been given in the vehicle bond graph for better spacing. Fig.4 and Fig.5 give the anti-roll bar schematic and bond graph.

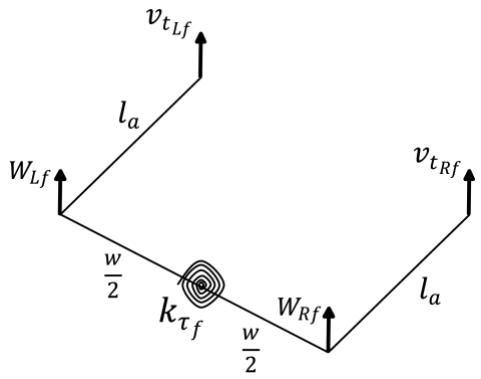

Figure 4. Anti-roll bar schematic

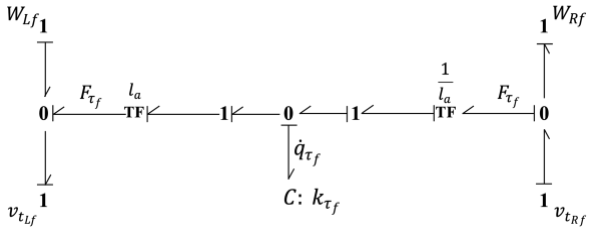

Figure 5. Front Anti-roll bar bond graph

With the bond graphs at hand, the equations of motion can be derived in a state-space where the state variables are the momenta associated with inertia elements and displacements associated with spring elements.

The translational equations of motion for the sprung mass are given as follows:

$$\dot{p}_U = M\dot{U} = -MW\omega_p + MV\omega_y + \left(F_{x_{Rf}} + F_{x_{Lf}}\right)\cos\delta - \left(F_{y_{Rf}} + F_{y_{Lf}}\right)\sin\delta + F_{x_{Rr}} + F_{x_{Lr}} \quad (1)$$

$$\dot{p}_V = M\dot{V} = -MU\omega_y + MW\omega_r + \left(F_{y_{Rf}} + F_{y_{Lf}}\right)\cos\delta + \left(F_{x_{Rf}} + F_{x_{Lf}}\right)\sin\delta + F_{y_{Rr}} + F_{y_{Lr}} \quad (2)$$

$$\dot{p}_W = m_s\dot{W} = -m_sV\omega_r + m_sU\omega_p - m_sg + F_{s_{Rf}} + F_{s_{Lf}} + F_{s_{Rr}} + F_{s_{Lr}} \quad (3)$$

Where p_U, p_V, p_W are the longitudinal, lateral, and vertical translational momenta of the sprung mass, respectively.

The Rotational momentum equations of motion for the sprung mass are:

$$\begin{aligned}\dot{p}_r = J_r\dot{\omega}_r = {} & J_p\omega_p\omega_y - J_y\omega_y\omega_p \\ & + h\Big(\big(F_{y_{Rf}} + F_{y_{Lf}}\big)\cos\delta \\ & + \big(F_{x_{Rf}} + F_{x_{Lf}}\big)\sin\delta + F_{y_{Rr}} + F_{y_{Lr}}\Big) \\ & + \frac{w}{2}\big(-F_{s_{Rf}} + F_{s_{Lf}} - F_{s_{Rr}} + F_{s_{Lr}}\big) \\ & - 2w\big(F_{\tau_f} + F_{\tau_r}\big) + \big(\tau_{t_{Rf}} + \tau_{t_{Lf}}\big)\sin\delta\end{aligned} \quad (4)$$

$$\begin{aligned}\dot{p}_p = J_p\dot{\omega}_p = {} & J_y\omega_y\omega_r - J_r\omega_r\omega_y + b\big(F_{s_{Rr}} + F_{s_{Lr}}\big) \\ & - a\big(F_{s_{Rf}} + F_{s_{Lf}}\big) \\ & - \big(\tau_{t_{Rf}} + \tau_{t_{Lf}}\big)\cos\delta - \big(\tau_{t_{Rr}} + \tau_{t_{Lr}}\big) \\ & + h\Big(\big(F_{y_{Rf}} + F_{y_{Lf}}\big)\sin\delta \\ & - \big(F_{x_{Rf}} + F_{x_{Lf}}\big)\cos\delta - \big(F_{x_{Rr}} + F_{x_{Lr}}\big)\Big)\end{aligned} \quad (5)$$

$$\begin{aligned}\dot{p}_y = J_y\dot{\omega}_y = {} & J_r\omega_r\omega_p - J_p\omega_p\omega_r \\ & + a\Big(\big(F_{y_{Rf}} + F_{y_{Lf}}\big)cos\,\delta \\ & + \big(F_{x_{Rf}} + F_{x_{Lf}}\big)sin\,\delta\Big) - b\big(F_{y_{Rr}} + F_{y_{Lr}}\big) \\ & + \frac{w}{2}\Big(\big(F_{x_{Rf}} - F_{x_{Lf}}\big)cos\,\delta \\ & + \big(F_{y_{Lf}} - F_{y_{Rf}}\big)sin\,\delta + (F_{x_{Rr}} - F_{x_{Lr}})\Big)\end{aligned} \quad (6)$$

Where p_r, p_p, p_y are the roll, pitch, and yaw angular momenta of the sprung mass.

Here in the equations of motion for the vehicle body, the Rf, Lf, Rr, Lr subscripts stand for right front, left front, right rear, and left rear, pertaining to each individual corner. Also F_x and F_y are longitudinal and lateral forces that come from a Dugoff tire model. Here δ is the front steered wheels angle, J is the moment of inertia with subscripts r, p, and y pertaining to roll, pitch, and yaw directions. M is the total vehicle mass, m_s is the sprung mass, and F_s are suspension forces pertaining to each corner. The vehicle body spatial velocities include U, V, W being the longitudinal, lateral, and vertical center of gravity velocities with $\omega_r, \omega_p, \omega_y$ being the roll, pitch, and yaw angular velocities around the vehicle's principal axes.

The vehicle model has been validated for random road input generation, vertical dynamics, and horizontal dynamics, respectively against ISO8608(Múčka 2017), Margolis et al.(Margolis and Nobles 1991), and CARSIM, which is a commercially established vehicle dynamics simulation software.

2.3. RIDE COMFORT METRIC

With both passenger model and vehicle model having been developed, we can now proceed to devise the novel, quantitative ride comfort metric. Decades-long studies have shown that back pain and discomfort is mostly associated with the lower lumbar spine(Katz 2006). In particular, the L5S1 and L4L5 discs are susceptible to the highest levels of trauma. Therefore, the said two joints are selected and their deviation from their most comfortable state, i.e. their static equilibrium, is considered as a discomfort index. As the passenger model is within a gravity field, every compliance element that has been modeled as a spring has a non-zero initial displacement value. The non-dimensional deviations from said initial displacements for the L5S1 and L4L5 joints are introduced as follows:

$$\begin{aligned}q^* = \frac{q - q_0}{q_0} \;\; ; \;\; & q \\ = \{ & q_{a_{L5S1}}, q_{s_{L5S1}}, q_{r_{L5S1}}, q_{a_{L4L5}}, q_{s_{L4L5}}, q_{r_{L4L5}}\}\end{aligned} \quad (7)$$

Here the a, s, and r subscripts denote axial, shear, and rotary displacements within the joints of interest.

The square of these non-displacement deviations is considered as a ride-discomfort measure. The next step is to calculate one combined ride-discomfort index using a weighted sum, as the contribution of each deviation to the total discomfort metric could be different.

To come up with individual weighting factors, non-dimensional energies were defined as the time integral of the square of the magnitude of the displacement deviation. Parseval's Theorem for

Fourier Transforms indicates an equivalence between time-domain and frequency domain for said energy signals.

$$E_i{}^* = \int_{-\infty}^{\infty} |q_i{}^*(t)|^2 dt = \frac{1}{2\pi} \int_{-\infty}^{\infty} |Q_i{}^*(\omega)|^2 d\omega$$

(8)

These $E_i{}^*$ energy signals were calculated for each direction. The simulation was run 100 times and the energies were normalized by their minimum value each time with the quotient being considered as the weighting factor for that particular direction.

$$E^* = \bigcup_{i=1}^{9} E_i{}^* \quad ; \quad w_i = \frac{E_i{}^*}{\min(E^*)}$$

(9)

It was found that the calculated weighting factors had a negligible standard deviation amidst the 100 runs and therefore the calculated weights could be employed in constructing the total cost function.

Now everything is ready to define the ride-comfort metric as follows.

$$A.R.C = \int_0^{\infty} \sum_{i=1}^{6} w_i {q_i}^{*2}\, dt$$

(10)

Where ARC stands for (First Author's initials) Ride Comfort, and the proposed ride comfort index will be henceforth known as the ARC. Building on the original hypothesis, a ride which corresponds to the smallest possible ARC would be most comfortable. The ARC is technically a measure of discomfort and therefore the lower the ARC, the more comfortable the ride. It is essential to address that the ARC is the integral of an always positive signal and therefore it ever increases and an appropriate controller would mitigate this increase as much as possible.

The expanded form of the ARC is given as follows.

$$A.R.C = \int_0^{\infty} \Big\{ \left(q^*{}_{a_{L5S1}}\right)^2 + 2.06\left(q^*{}_{s_{L5S1}}\right)^2 + 2.33\left(q^*{}_{r_{L5S1}}\right)^2 + 1.27\left(q^*{}_{a_{L4L5}}\right)^2 + 8.30\left(q^*{}_{s_{L4L5}}\right)^2 + 5\left(q^*{}_{r_{L4L5}}\right)^2 \Big\} dt$$

(11)

2.4. CONTROLLER DESIGN

The proposed control strategy for optimizing passenger ride comfort in a moving vehicle is to control the seats instead of the entire suspension. Fig.6 gives a schematic of the seat control and actuator locations. Three force actuators are assumed to have been placed in those locations where the seat passively exerts force on the passenger body, next to the passive springs and dampers already in place, namely being in the seat's hip cushion, lumbar backrest, and thoracic backrest.

Given that the equations of motion are given in a state-space, a state-variable feedback control strategy seems appropriate. In order for such strategy to work, the state variables are required. Since there is no direct access to the state variables, an observer is required which could estimate the state variables from certain sensor outputs. For the observing sensors, it is assumed that displacement sensors are placed right next to the actuators, a control/estimation technique known as colocation.

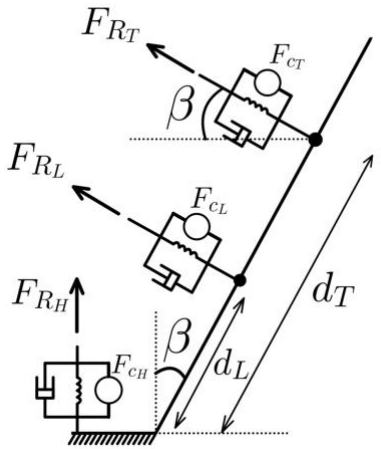

Figure 6. Schematic of actuator/sensor location and control/estimation strategy

For the next step, the original, nonlinear system of equations are linearized around their equilibrium position. Fig.7 shows a comparison of the response of the original nonlinear system and the linearized system to a random road input for two of the main signals employed to construct the ARC cost function.

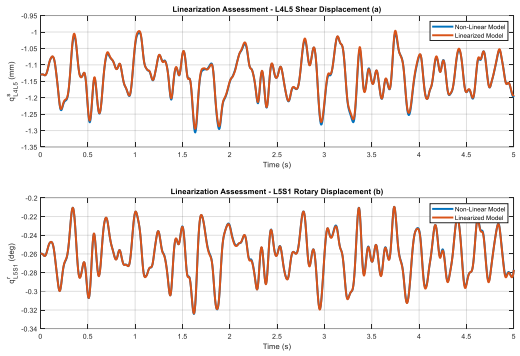

Figure 7. Comparison of the linearized system to the original nonlinear system

As is noticed in Fig.7, the linearized system tracks the response of the original, nonlinear system with high accuracy. Therefore, the linearized model can be trusted in designing a controller and an observer.

A Linear Quadratic cost function has been proposed and a Linear Quadratic Regulator (LQR) is used for the control of the 3 actuators. The LQR algorithm gives the state-gain matrix K such that when multiplied by the state vector yields commands to the actuators that will minimize the quadratic cost function (Lancaster and Rodman 1995). The quadratic cost function is given as follows.

$$J = \int_0^\infty (x^T Q x + u^T R u + 2x^T N u) dt$$

$$\vec{u} = -K\vec{x} \;\rightarrow\; J_{min}$$

(12)

Here J is the total cost function, Q and R are weighting matrices for the states and inputs, respectively, and N is a weighting matrix for any non-linear cross term in the cost function that might include the product of a state and an input. Once the gain matrix K is found, assuming one has access to the states, then $-K\vec{x}$ input will ensure the cost function would arrive at a global minimum.

The cost function is re-written in terms of ARC and the specified inputs.

$$J = \int_0^\infty \left\{ \sum_{i=1}^{6} Q_i {q_i}^{*2} + R_1 {F_{c_H}}^2 + R_2 {F_{c_L}}^2 + R_3 {F_{c_T}}^2 \right\} dt = ARC + \int_0^\infty \left(R_1 {F_{c_H}}^2 + R_2 {F_{c_L}}^2 + R_3 {F_{c_T}}^2 \right) dt$$

(13)

The Q_i weights are selected to match the found weightings for the ARC and the R_i weights are selected such that ARC is minimized while not consuming excessive energy.

Once the LQR design is complete, the observer will be designed using a Kalman Filter(Welch 2020). With the estimated states at hand, the state-space equations for the aggregated system become:

$$\dot{x} = Ax + Bu \;\;,\;\; y = Cx \;\;,\;\; u = -K\hat{x}$$

$$\dot{\hat{x}} = A\hat{x} + Bu + L(y - \hat{y}) \;\;,\;\; \hat{y} = C\hat{x} \;\;,\;\; u = -K\hat{x}$$

(14)

Here A and B are the same system matrices from the linearization, C is the matrix that associates the sensor outputs with the system states, and L is the observer gain matrix which determines the performance of the estimator to be designed, i.e., how fast can the observed $\hat{x}$ states track the actual x states. Fig.8 shows how the observer tracks the states once a non-zero initial condition is forced upon the system.

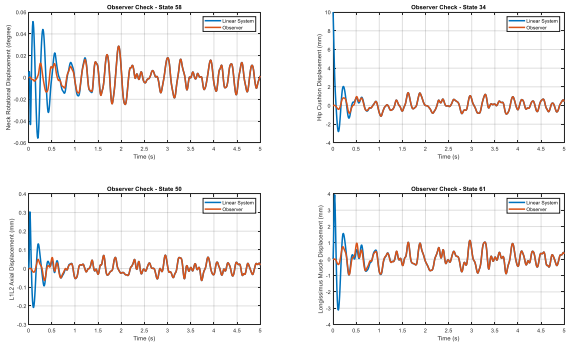

Figure 8. Checking the observer performance for four arbitrary states

It can be seen in Fig.8 that the observer manages to track the states adequately after half a second. Therefore, the observer can be trusted to provide

the state-variables for the state-variable feedback control.

3. RESULTS AND DISCUSSION

Once the observer-based controller is put in place, its performance in mitigating the ARC cost function can be assessed. Fig. 9 shows the performance of the controlled system against the passive system for the ARC cost function.

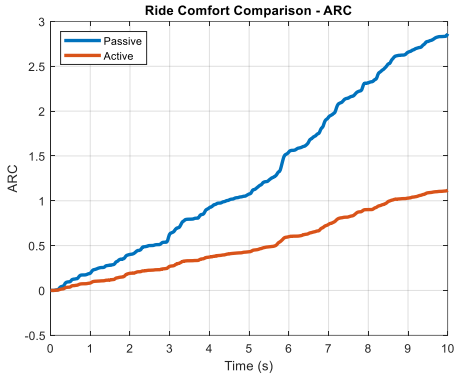

Figure 9. Comparison of the controlled system's performance against the passive system

It can be noticed in Fig.9 that the controller has managed to reduce the ARC by almost 60% which shows that the controller has mitigated the internal dynamic deviations of the passenger model and therefore enhanced ride comfort by 60%.

The next step is to check the amount of the required power and force for the actuators which are shown in Fig. 10.

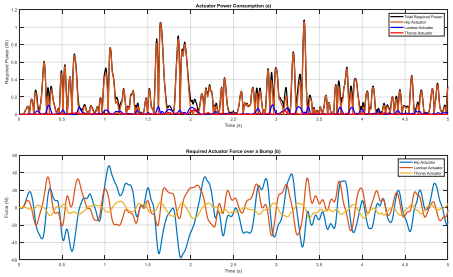

Figure 10. Input power and force requirements for the actuators

It can be seen in Fig.10 that both the power consumption and the force input requirements for the actuators are reasonable.

To ensure the controller's performance, the system is also exposed to a large transient input such as a rough bump like the one shown in Fig.11.

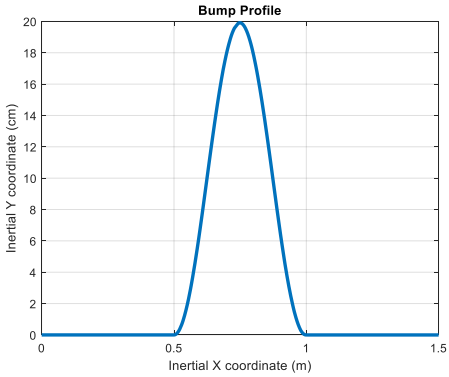

Figure 11. Profile of a large transient bump input

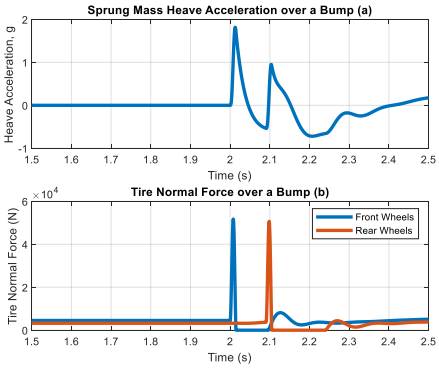

Figure 12. Heave acceleration and tire normal force in response to going over the harsh bump

Fig.12 shows that once the vehicle traverses the large bump, the tires momentarily lose contact with the ground and excessive heave accelerations are experienced.

Again, the controller's performance was assessed against the large bump input. Fig. 13 gives the ARC cost function for the controlled system vs the passive system as the vehicle goes over the harsh bump.

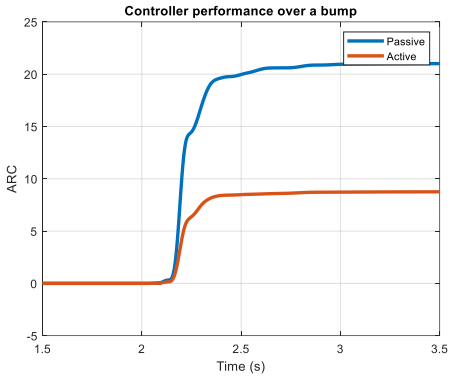

Figure 13. Controller performance in mitigating the ARC over a bump

It can be noticed in Fig.13 that the controller has performed against transient, sudden inputs just as well as steady, random inputs.

The power consumption and force requirements for traversing the bump in given in Fig.14

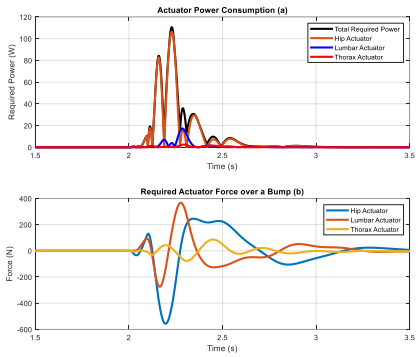

Figure 14. Power and force requirements for the controlled system when traversing a bump

Fig. 14 shows that while power/force requirements for the controller when traversing a harsh bump are larger than when going over a random road, they are still reasonable.

4. CONCLUSION

In order to come up with a quantitative, non-subjective ride comfort metric, one was devised as a comfort cost function according to passenger biomechanics which came off of a nonlinear planar analytical model of a vehicle's passenger. To mitigate the cost function known as the ARC, the non-linear passenger model was linearized, and an observer-based state variable feedback controller was designed to reduce the ARC which corroborates with better ride comfort. It was gathered that the controller can reduce the ARC by 60% when going over a random road without consuming excessive power or force. If exposed to extreme road inputs such as a rough bump, it was observed that the controller can still reduce the ARC by 50%, despite requiring more power and force.

REFERENCES

Akbari, A. and D. Margolis (2021). A Bond Graph Representation of the Sagittal Spine for Estimation of Ride Comfort. 2021 International Conference on Bond Graph Modeling and Simulation, ICBGM 2021.

Akbari, A. and D. Margolis (2024). "A biomechanical model of a vehicle passenger in the sagittal plane." Heliyon.

BSI (1987). Guide to measurement and evaluation of human exposure to whole-body mechanical vibration and repeated shock. BS6841, British Standards Institution.

Da Silva, M. G. (2002). "Measurements of comfort in vehicles." Measurement Science and Technology **13**(6): R41.

Dieckmann, D. (1958). "A study of the influence of vibration on man." Ergonomics **1**(4): 347-355.

Els, P. (2005). "The applicability of ride comfort standards to off-road vehicles." Journal of Terramechanics **42**(1): 47-64.

Enders, E., G. Burkhard, F. Fent, M. Lienkamp and D. Schramm (2019). "Objectification methods for ride comfort." Forschung im Ingenieurwesen **83**(4): 885-898.

Fothergill, L. and M. Griffin (1977). "The evaluation of discomfort produced by multiple frequency whole-body vibration." Ergonomics **20**(3): 263-276.

ISO (1997). Shock evaluation of human exposure to whole-body vibration. ISO 2631, International Organization for Standardization.

Jacklin, H. (1936). "Human reactions to vibration." SAE Transactions: 401-408.

Jones, A. and S. DJ (1974). "A scale of human reaction to whole body, vertical, sinusoidal vibration."

Katz, J. N. (2006). "Lumbar disc disorders and low-back pain: socioeconomic factors and consequences." JBJS **88**(suppl_2): 21-24.

Lancaster, P. and L. Rodman (1995). Algebraic riccati equations, Clarendon press.

Margolis, D. L. and C. M. Nobles (1991). "Semi-active heave and roll control for large off-road vehicles." SAE transactions: 467-476.
Múčka, P. (2017). "Simulated road profiles according to ISO 8608 in vibration analysis." Journal of Testing and Evaluation **46**(1): 405-418.
Oborne, D. (1976). "A critical assessment of studies relating whole-body vibration to passenger comfort." Ergonomics **19**(6): 751-774.
Oborne, D. (1977). "Vibration and passenger comfort." Applied Ergonomics **8**(2): 97-101.
Oborne, D. and M. Clarke (1974). "The determination of equal comfort zones for whole-body vibration." Ergonomics **17**(6): 769-782.
Pradko, F. and R. A. Lee (1966). Vibration comfort criteria, SAE Technical Paper.
Reiher, H. and F. Meister (1932). "Die Empfindlichkeit des Menschen gegen Stöße." Forschung auf dem Gebiet des Ingenieurwesens A **3**: 177-180.
Sharma, R. C. (2016). "Evaluation of Passenger Ride Comfort of Indian Rail and Road Vehicles with ISO 2631-1 Standards: Part 1-Mathematical Modeling." International Journal of Vehicle Structures & Systems (IJVSS) **8**(1).
Sperling, E. and C. Betzhold (1957). Contribution to evaluation of comfortable running of railway vehicles. Bulletin of the International Railway Congress Association.
VDI (2002). Human exposure to mechanical whole-body vibration. VDI2057, Association of German Engineers.
Wang, C., X. Zhao, R. Fu and Z. Li (2020). "Research on the comfort of vehicle passengers considering the vehicle motion state and passenger physiological characteristics: improving the passenger comfort of autonomous vehicles." International journal of environmental research and public health **17**(18): 6821.
Welch, G. F. (2020). "Kalman filter." Computer Vision: A Reference Guide: 1-3.
Yang, Y., W. Ren, L. Chen, M. Jiang and Y. Yang (2009). "Study on ride comfort of tractor with tandem suspension based on multi-body system dynamics." Applied Mathematical Modelling **33**(1): 11-33.

AUTHOR BIOGRAPHY

Ali Akbari received his BSc. and MSc. Certificates from Sharif University of Technology in Tehran, Iran and his Ph.D. from the University of California, Davis. His research interests are passenger biomechanics and vehicle dynamics and controls.

Donald Margolis is a professor of mechanical and aerospace engineering at the University of California, Davis. He received his BSc. From Virginia Tech university and got his MSc. and Ph.D. from Massachusetts Institute of Technology. He has over 50 years of industrial and academic experience and his research interests include vehicle dynamics and controls, vibration control, and the simulation and modeling of dynamic systems.